

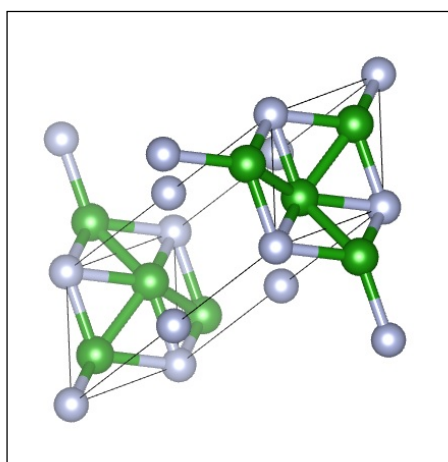


## Boron Activity in Metal Containing Materials

O. Murat Ozkendir<sup>1,2,✉</sup>

Received: 07 February 2020 / Accepted: 17 February 2020 / Published Online: 27 March 2020

© SAMI Publishing Company (SPC) 2020



### ABSTRACT

Boron is one of the most popular materials in recent technologies due to its potential to emerge desired technological results. Many attempts have been done to understand the boron activity in crystal media or on the electronic properties of the materials to understand the mechanisms as a result of interesting molecular interplays between neighboring atoms. In the most studies, boron atoms did not have the main role in the first steps of the scientific study where it took place. However, mostly it has become the key element and the main role player that is reported as the interesting results of the research. In this study, the background activities of the boron atom are investigated regarding its roles as dopant or substitution element.

**Keywords:** Crystal structure; Electronic structure; Boron; Doping.

### Introduction

Boron is a special element located in group III of the periodic table with both metallic and nonmetallic properties, i.e., metalloid. In this group, boron is the only element that shows non-metallic properties. Also, its physical and chemical properties are unique due to consisting of two electron bonds, a high melting point (2349 K), high hardness and desired chemical stability [1-5]. These properties make it a multifunctional element for use in every aspect of the technology such as; nuclear technology, nutrients for plants, treatment for cancer cells, semiconductor

technology or storage device technology [6]. Boron crystallizes in tetragonal (Fig. 1a) or trigonal (rhombohedral) geometry (Fig. 1b). Due to interesting results which have been achieved for the boron-containing elements over the last 20 years, boron attracted attentions of the scientists from various disciplines [7-10]. Especially, the oxide complexes of boron attracted considerable attentions of research on optoelectronic devices, storage devices or medical applications. The medical treatment processes with boron and boron complex have many varieties of applications. Boron Neutron Capture Therapy

✉ Corresponding author.

E-mail address: [ozkendir@gmail.com](mailto:ozkendir@gmail.com) (O.M. Ozkendir)

<sup>1</sup> School of Graduate Programs, Tarsus University, Tarsus, Turkey

<sup>2</sup> Department of Energy Systems Engineering, Faculty of Technology, Tarsus University, Tarsus, Turkey

(BNCT) with nanomaterials is one of the well-known methods, which is a powerful and broadly applicable radiation therapy using boron-enriched

compounds. In this treatment process, a non-invasive approach for selective destruction of cancer cells is aimed [11].

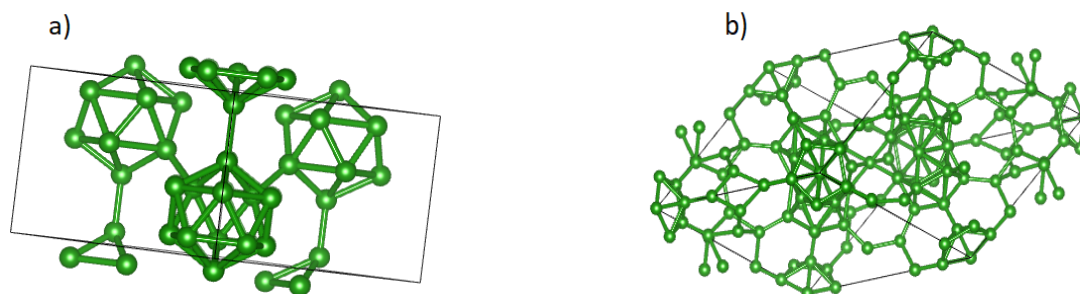


**Fig. 1.** The crystal structures of the elemental boron; a) Tetragonal and b) Trigonal.

In most research works, the boron atom is focused on its influence on the electronic interplay with its neighboring atoms to obtain a molecular structure with desired electronic, crystal or magnetic properties. In this manner, so many reports have been published on the influence of boron in its environment [6, 12]. Both theoretical and experimental approaches confirmed the interesting nature of the boron and its oxides by showing a clear path for boron complexes in further technological applications that should be used by the scientists. For the use of boron atom, several studies have been focused on exploration of medical applications. Nakagawa and co-workers [13] suggested that the boron-containing apatite (BAp) ceramics could be used as useful biomaterials known as immune ceramics activating the immune system itself without any need to rely on expensive proteins.

The key knowledge on the elemental discoveries lays on the study of the electronic properties, which gives the information of what element can do or yield when treated under different circumstances. The knowledge of “How?” gives us clues about its electronic states. Because the only way of an atom to say “Hello!” to others is to shake hands via its valence electrons. Thus, in this study, we will have a short look at different types of boron complexes by their electronic structure and its interplay with the neighbors by the XAS (x-ray

absorption spectroscopy) calculations. The XAS technique is a popular method for determining the local geometric and/or electronic structure of materials. For the experimental studies, synchrotron radiation facilities are used and with an extra range excitation, it is called XAFS (x-ray absorption fine structure) spectroscopy. The XAS technique is an element-specific technique and the samples can be in solid, liquid (solutions), or in the gas phase.

## A general Outlook to Most Studied Boron Structures

### Boron Nitride (BN) Structure

Boron nitride is one the most studied member of the boron complexes due to its properties such as; high tensile strength, high thermal conductivity, high bandgap (~6 eV), high neutron absorption cross-section, resistance to oxidation in air and independent of chirality [14]. Especially, the BN nanotube has been mostly used to improve mechanical properties of the metal composites and as a shield for satellites and astronauts for neutron radiation, dielectrics in use of nanoelectronics and for medical imaging. The boron nitride crystal structure is sketched in Fig. 2 [15].

In the BN nanostructures, boron atom possess  $B^{3+}$  ionic state, while nitrogen atom possess  $N^{3-}$  ionic state and crystallizes in trigonal geometry with the

“p-3m1” space group. The BN nanostructures are supposed to be ionic nanostructures in contrast with non-ionic carbon ones [16-18].

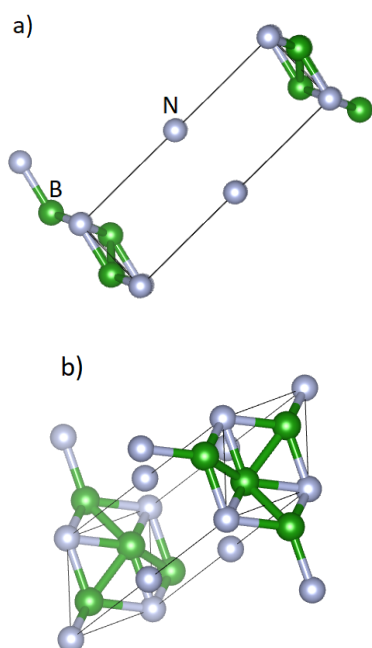


**Fig. 2.** Boron nitride crystal structure, aspects from different perspectives a) x-axis b) xyz-conjunction.

The probe of electronic interplay between boron and the nitrogen atoms in BN crystals, XAS (x-ray absorption spectroscopy) calculations are performed using the FEFF 8.2 commercial code [19]. The FEFF code uses crystallographic data as the input file for calculations. The input data was prepared for 10 Å cluster of trigonal BN crystal containing 452 atoms (B, N) and one boron atom was selected as a photoelectron emitter. The calculated boron K-edge spectra are given in Fig. 3. The XAS spectroscopy is sensitive to atomic environments and can give rich data on the electronic structure with chemical bonding properties. Boron K-edge peak is a result of the 1s core electrons' transition to unoccupied 2p levels of the  $B^{3+}$  ions and has a maximum at 192.8 eV. This sharp “Whiteline” peak is attributed to the  $\pi^*$  anti-bonding orbital states [20]. The sharp peak is due to the low photon-electron cross-section on the z-axis where photons are incoming and yield a

narrow sharp peak ( $\pi^*$ ). However, when the photons and electrons are in resonance and interact along with the incoming photons, they yield broad absorption peaks ( $\sigma^*$ ). The second peak beyond the Whiteline peak is a result of the transitions from the core levels to  $\sigma^*$  states. The XAS spectra may contain a pre-edge structure, at which an overlapping between neighboring electrons and levels will be occurred. In such a case, a pre-edge peak may appear just below the main absorption edge to show if a forbidden transition occurs which does not obey the quantum selection rules. Here, the valence levels of both B and N are the 2p levels and  $1s \rightarrow 2p$  obeys the quantum selection rules. Besides, the pre-edge also works as an indicator of the crystal distortions, asymmetries or any unusual phenomena in the crystals.

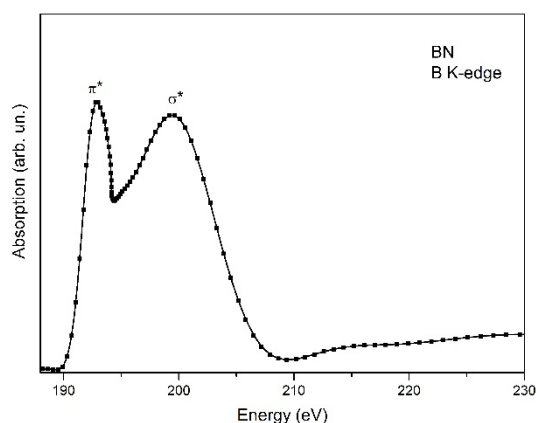


**Fig. 3.** Boron K-edge absorption spectra of the boron nitride.

### Boron Oxide ( $B_2O_3$ ) Structure

Boron oxide ( $B_2O_3$ ) is the most popular form of the boron oxide family. It has white color and granular in texture. It is widely used for glass production like optical lenses, glass-ceramic composite materials, and electronic glasses. Thermal resistance and mechanical strength are two main reasons for use of  $B_2O_3$  oxide in industrial fields.  $B_2O_3$  crystallizes in trigonal geometry and the "P3121" space group (given in Fig. 4).

With the unusual electronic properties and its outcomes in the recent technological applications,

studies on boron oxides and boron-containing materials became popular. Boron and its interplay with oxygen atoms during building the molecular bonding between boron and oxygen are the most popular subjects focused to find out the background of all unusual properties. In one of the studies, Burkholder and Andrews [21, 22] reported that boron atoms are highly exothermic and produce exclusively BO when interacted with the reaction  $O_2$  gas. One of the major problems encountered during boron studies is the high refractory of the boron atoms and due to this problem, the difficulties in producing boron materials were tried to overcome by using boric acid [22]. Studies on boron oxide materials are mainly focused on the  $B_2O_3$  material.

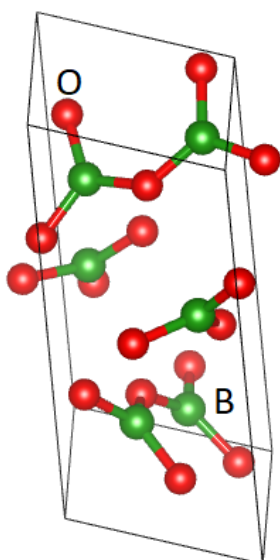


**Fig. 4.** Crystal Structure of the boron oxide ( $B_2O_3$ ) material.

In another study, Li and Xue [23] have probed the hexavalent chromium formation mechanism via the enrichment form of chromium in stainless-steel slag by using boron oxide. They determined that a lower addition of boron oxide content made a lower emission of hexavalent chromium from the waste of chromium.  $B_2O_3$  has also a vast field of technological applications in medical treatments; radioluminescence properties, use in bioactive glasses for medical issues, gamma-ray attenuation properties, etc. [24-27]. Since 1950s,

boron derivatives have been used in the clinical trials against tumor treatments. Besides the desired optical properties, boron oxide materials have been used in the preparation of energy storage devices in recent years. The lithium-ion batteries are the most and efficiently used energy storage devices in every area of technology where mobility is needed. In this manner, Ozkendir and co-workers [28, 29] published several reports on the boron activities and influences on the battery cathode or electrolyte materials. Recently, it is reported that in the studied boron substituted  $Li_2MnO_3$  (known as inactive) cathode material, boron atoms acted as a landmark for the parent oxides by forming  $LiBO_2$  crystal domains. And, due to the lack of oxygen atoms around, the manganese atoms were determined to build up cubic  $LiMn_2O_4$  crystal structure. It was astonishing because the system turned into a composite " $Li_2MnO_3$ - $LiBO_2$ - $LiMn_2O_4$ " cathode material with 10% boron substitution, which was reported with good electrochemical properties in the literature with the general formula  $xLi_2MnO_3 \cdot (1-x)LiMn_2O_4$ . Ozkendir [28] reported interesting phenomena in boron-containing materials as the effect of boron on its environment.

To understand the electronic interplay between boron and oxygen, the calculation for the  $B_2O_3$  material was performed. Ionic states of the ions are;  $B^{3+}$  and  $O^{2-}$  in the  $B_2O_3$  material. For the XAS (x-ray absorption spectroscopy) calculations, the input file for trigonal  $B_2O_3$  with "P3121" space group is performed using the commercial code FEFF 8.2 [19]. The input data was prepared for 10 Å cluster crystal containing 562 atoms (B, O) and one boron atom was selected as a photoelectron emitter. The calculated boron K-edge spectra are given in Fig. 5.

Like the XAS data given in Fig. 3, boron K-edge from  $1s \rightarrow 2p$  transition has a Whiteline peak with a maximum at 192.4 eV and this peak is attributed to the  $\pi^*$  anti-bonding orbital states [20]. However, the width of the boron K-edge has a

broadening in width, which is addressed to the increase in divergence of tetrahedral bond length between boron and oxygen [30]. The weak peak structure beyond the Whiteline peak at 202.4 eV is a result of the transitions from the core levels to  $\sigma^*$  states.

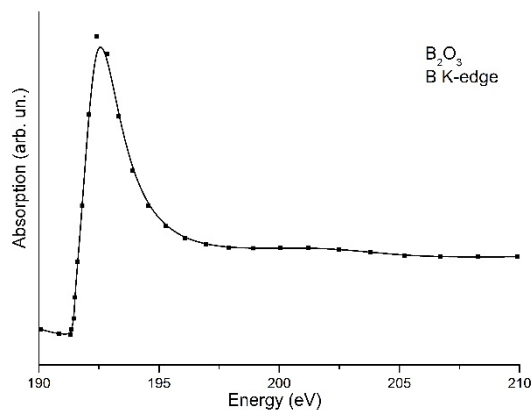


**Fig. 5.** Boron K-edge absorption spectra of the boron oxide ( $B_2O_3$ ).

### Uranium Tetra Boride ( $UB_4$ ) Structure

Uranium is a member of the actinide group which is also known with 5f electronic states. Metals of this family are also called as the 5f transition metals and have an important role/place in nuclear technologies. Beside these features, they are also studied for their electrical, electronic and also magnetic properties.  $UB_4$  is one of the known intermetallic compounds and behaves as a Pauli paramagnet [31-34]. The uranium boride ( $UB_4$ ) crystal forms in tetragonal geometry in "P4/mbm" space group as given in Fig. 6 with different angular aspects. The electronic structure studies performed by Yamamoto and co-workers [35] have shown that  $UB_4$  is a moderate heavy-fermion compound with determined values ( $\gamma=24.9$  mJ/K<sup>2</sup>,  $m_{cyclotron}= 3-14.1 m_0$ ) and reported to have a high Kondo temperature. The thermoelectric properties of  $UB_4$  with different isotopic compositions are reported about 4–6  $\mu$ V/K at room temperature and decreased with decreasing temperature [35]. From the studies in the literature, uranium tetraboride is concluded to have a poor thermoelectric material due to

metallic properties like low thermoelectric power and large electrical resistivity.

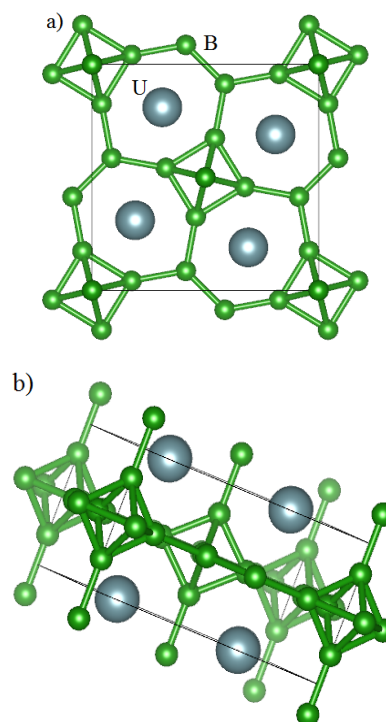


**Fig. 6.** Uranium tetra boride crystal structure, aspects from different perspectives; a) z-axis and b) x-axis.

All properties shown by the  $UB_4$  are related to the electronic interactions between the neighboring U and B atoms. The electronic interplay of these elements should have an interesting property. Because, according to the quantum selection rules, the valence states of U (5f) and B (2p) cannot interact directly, i.e.,  $\Delta l = \pm 1$ . Thus, electronic structure background plays an important role in bonding. Metallic uranium has the electronic configuration [Rn]  $5f^3 6d^1 7s^2$ , while boron has [He]  $2s^2 2p^1$ . The f-level is unoccupied on uranium atoms and p-level is unoccupied on the boron atoms. That means the p-level of the boron atoms cannot interact with uranium atom directly due to the unoccupied f-levels, but indirectly with d-levels. So, mixed f- and d-level can bind with the p-electrons of boron and a hybridized molecular band should be built. While f-symmetry in the molecular band avoids the p-electrons from the band, d-symmetry attracts p-electrons to interact

when excited. Thus, a pre-edge structure may appear due to given details, well above. The boron K-edge XAS calculation data is given in Fig. 7. The input data was prepared for 10 Å cluster crystal containing 353 atoms (U, B) and one boron atom was selected as a photoelectron emitter.

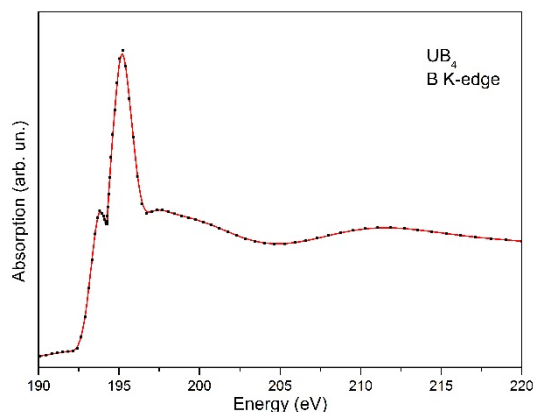


**Fig. 7.** Boron K-edge absorption spectra of the uranium tetra boride ( $UB_4$ ).

The calculated absorption spectra began to rise at 192 eV and has sharp shoulder like pre-edge just below the main edge at 193.8 eV. This edge has the properties of a pre-edge and so powerful due to the high number of the unoccupied states on d-level. The main peak has the maximum at 195.2 eV which is attributed to the  $\pi^*$ -antibonding. The electronic structure pointed out that, the rich quantum symmetry in the molecular bond built between uranium and the boron atoms can support interesting molecular interplays that may

yield fruitful properties for the technological applications.

## Conclusion

In this study, the characteristics of boron atom and its different forms are analyzed via its electronic structure properties by the calculations. The calculations were done for the boron compounds at room temperatures and aimed to enlighten the background mechanism appear as a result of electronic interactions to build up new molecular bands. In this manner, electronic properties of the boron nitride (BN), boron oxide ( $B_2O_3$ ) and uranium tetra boride ( $UB_4$ ) materials were investigated. The electronic structure studies were carried with the boron K-edge absorption spectra which were calculated using the commercial code FEFF 8.2. Boron K-edge was determined to have slight changes on the photon energy value of 192~195 eV according to the bonded element. Typical Whiteline on the K-edge spectra welcomes and it is attributed to  $\pi^*$ -antibonding, while in some spectra (BN) a Gaussian broad peak are located just above the Whiteline and attributed to  $\sigma^*$ -antibonding. When boron built up a molecule with light elements (N, O) no pre-edge structure observed. However, with obtaining a compound with a heavier element (U), a powerful pre-edge feature observed due to the U 5f6d/O 2p hybridization.

## References

1. Tsagareishvili GV, Tavadze FN. Boron crystals: Preparation, structure and properties. Prog. Cryst. Growth Charact. 1988;16:341-365.
2. Emin D. Icosahedral boron-rich solids. Phys. Today 1987;40:55-62.
3. Gaule GK. Boron: preparation, properties, and application. Plenum Press; New York: 1965.
4. Ulas A, Kuo KK, Gotzmer C, Ignition and combustion of boron particles in fluorine-containing environments. Combust. Flame 2001;127:1935-1957.
5. Tian Y, Guo Z, Zhang T, Lin H, Li Z, Chen J, Deng S, Liu F. Inorganic boron-based nanostructures: Synthesis, optoelectronic properties, and prospective applications. Nanomater. 2019;9:538.
6. Ozkendir OM, Harfouche M, Ulfat I, Kaya Ç, Celik G, Ates S, Aktas S, Baveghar H, Colak T. Boron activity in the inactive  $Li_2MnO_3$  cathode material. J. Electron Spect. Related Phenom. 2019;235:23-28.
7. Mirzaei M, Hadipour NL, Abolhassani MR. Influence of C-doping on the B-11 and N-14 quadrupole coupling constants in boron-nitride nanotubes: A DFT study. Z. Naturforsch. A 2007;62:56-60.
8. Mirzaei M. Density functional study of defects in boron nitride nanotubes. Z. Phys. Chem. 2009;223:815-823.

9. Mirzaei M. Calculation of chemical shielding in C-doped zigzag BN nanotubes. *Monatsh. Chem.* 2009;140:1275-1278.
10. Bagheri Z, Mirzaei M, Hadipour NL, Abolhassani MR. Density functional theory study of boron nitride nanotubes: calculations of the N-14 and B-11 nuclear quadrupole resonance parameters. *J. Comput. Theor. Nanosci.* 2008;5:614-618.
11. Singh A, Kim BK, Mackeyev Y, Rohani P, Supriya DM, Swihart MT, Krishnan S, Paras NP. Boron-nanoparticle-loaded folic-acid-functionalized liposomes to achieve optimum boron concentration for boron neutron capture therapy of cancer. *J. Biomed. Nanotechnol.* 2019;15:1714-1723.
12. Ozkendir OM, Gunaydin S, Mirzaei M. Electronic structure study of the LiBC<sub>3</sub> borocarbide graphene material. *Adv. J. Chem. B* 2019;1:37-41.
13. Nakagawa D, Nakamura M, Nagai S, Aizawa M. Fabrications of boron-containing apatite ceramics via ultrasonic spray-pyrolysis route and their responses to immunocytes. *J. Mater. Sci.* 2020;31:20.
14. Marincel DM, Adnan M, Ma J, Bengio EA, Trafford MA, Kleinerman O, Kosynkin DV, Chu SH, Park C, Hocker SJ, Fay CC. Scalable purification of boron nitride nanotubes via wet thermal etching. *Chem. Mater.* 2019;31:1520-1527.
15. Momma K, Izumi F. VESTA 3 for three-dimensional visualization of crystal, volumetric and morphology data. *J. Appl. Cryst.* 2011;44:1272-1276.
16. Mirzaei M, Hadipour NL, Seif A, Giahi M. Density functional study of zigzag BN nanotubes with equivalent ends. *Physica E* 2008;40:3060-3063.
17. Mirzaei M, Mirzaei M. Electronic structure of sulfur terminated zigzag boron nitride nanotube: A computational study. *Solid State Sci.* 2010;12:1337-1340.
18. Mirzaei M. The NMR parameters of the SiC-doped BN nanotubes: a DFT study. *Physica E* 2010;42:1954-1957.
19. Ankudinov AL, Rehr JJ. Relativistic calculations of spin-dependent x-ray-absorption spectra. *Phys. Rev. B* 1997;56:R1712.
20. Lee SH, Jeong H, Okello OF, Xiao S, Moon S, Kim DY, Kim GY, Lo JI, Peng YC, Cheng BM, Miyake H. Improvements in structural and optical properties of wafer-scale hexagonal boron nitride film by post-growth annealing. *Sci. Rep.* 2019;9:1-8.
21. Hanner AW, Gole JL. Evidence for ultrafast V-E transfer in boron oxide (BO). *J. Chem. Phys.* 1980;73:5025-5039.
22. Burkholder TR, Andrews L. Reactions of boron atoms with molecular oxygen. Infrared spectra of BO, BO<sub>2</sub>, B<sub>2</sub>O<sub>2</sub>, B<sub>2</sub>O<sub>3</sub>, and BO-2 in solid argon. *J. Chem. Phys.* 1991;95:8697-8709.
23. Li W, Xue X. Emission reduction research and formation of hexavalent chromium in stainless steel smelting: Cooling rate and boron oxide addition effects. *Process Safety Environ. Protect.* 2019;122:131-143.
24. Jiang C, Deng P, Zhang J, Gan F. Radioluminescence of Ce<sup>3+</sup>-doped B<sub>2</sub>O<sub>3</sub>-SiO<sub>2</sub>-Gd<sub>2</sub>O<sub>3</sub>-BaO glass. *Phys. Lett. A* 2004;323:323-328.
25. Prasad NV, Annapurna K, Hussain NS, Buddhudu S. Spectral analysis of Ho<sup>3+</sup>: TeO<sub>2</sub>-B<sub>2</sub>O<sub>3</sub>-Li<sub>2</sub>O glass. *Mater. Lett.* 2003;57:2071-2080.
26. Singh N, Singh KJ, Singh K, Singh H. Gamma-ray attenuation studies of PbO-BaO-B<sub>2</sub>O<sub>3</sub> glass system. *Rad. Measur.* 2006;41:84-88.
27. Saranti A, Koutselas I, Karakassides MA. Bioactive glasses in the system CaO-B<sub>2</sub>O<sub>3</sub>-P<sub>2</sub>O<sub>5</sub>: preparation, structural study and in vitro evaluation. *J. Non-Cryst. Solids* 2006;352:390-398.
28. Ozkendir OM. Determination of the atomic coordinations of the substituted light atoms in materials. *J. Optoelect. Adv. Mater.* 2019;21:357-360.
29. Ozkendir OM, Ates S, Celik G, Klysubun W. Influence of boron substitution on the crystal and electronic properties of LiCrO<sub>2</sub> battery cathode. *Metal. Mater. Transact. A* 2017;48:2993-2998.
30. Fleet ME, Liu X. Boron K-edge XANES of boron oxides: tetrahedral B-O distances and near-surface alteration. *Phys. Chem. Miner.* 2001;28:421-427.
31. Galatanu A, Yamamoto E, Haga Y, Ōnuki Y. Magnetic behaviour of UB<sub>4</sub> at high temperatures. *Physica B* 2006 M;378:999-1000.
32. Yamamoto E, Haga Y, Honma T, Inada Y, Aoki D, Hedo M, Yoshida Y, Yamagami H, Ōnuki Y. De Haas-van alphen effect and energy band structure in UB<sub>2</sub>. *J. Phys. Soc. Japan* 1998;67:3171-3175.
33. Umehara I, Kurosawa Y, Nagai N, Satoh K, Kasaya M, Iga F. Magnetoresistance and de Haas-van alphen effect in UB<sub>12</sub>. *J. Phys. Soc. Japan* 1990;59:2320-2323.
34. Yamamoto E, Honma T, Haga Y, Inada Y, Aoki D, Tokiwa Y, Suzuki N, Miyake K, Ōnuki Y. Magnetoresistance and de Haas-van alphen effect in UB<sub>4</sub>. *J. Phys. Soc. Japan.* 1999;68:3347-3351.
35. Nishi Y, Arita Y, Terao K, Matsui T, Nagasaki T. Boron isotope effects on the thermoelectric properties of UB<sub>4</sub> at low temperatures. *J. Nucl. Mater.* 2001;294:209-211.

**How to cite this article:** Ozkendir OM. Boron Activity in Metal Containing Materials. *Adv. J. Chem. B.* 2020;2(2):48-54. doi: [10.33945/SAMI/AJCB.2020.2.2](https://doi.org/10.33945/SAMI/AJCB.2020.2.2)